



Article

Reconstruction of Full-Length circRNA Sequences Using Chimeric Alignment Information

Md. Tofazzal Hossain ^{1,2,3}, Jingjing Zhang ^{1,2}, Md. Selim Reza ^{1,2}, Yin Peng ^{4,*}, Shengzhong Feng ¹ and Yanjie Wei ^{1,*}

- ¹ Center for High Performance Computing, Joint Engineering Research Center for Health Big Data Intelligent Analysis Technology, Shenzhen Institute of Advanced Technology, Chinese Academy of Sciences, Shenzhen 518055, China; tofazzal.stat@gmail.com (M.T.H.); zhangjj@siat.ac.cn (J.Z.); selim@siat.ac.cn (M.S.R.); sz.feng@siat.ac.cn (S.F.)
- ² School of Computer Science and Technology, University of Chinese Academy of Sciences, Beijing 100049, China
- ³ Department of Statistics, Bangabandhu Sheikh Mujibur Rahaman Science and Technology University, Gopalganj 8100, Bangladesh
- ⁴ Department of Pathology, The Shenzhen University School of Medicine, Shenzhen 518060, China
- * Correspondence: ypeng@szu.edu.cn (Y.P.); yj.wei@siat.ac.cn (Y.W.)

Abstract: Circular RNAs (circRNAs) are RNA molecules formed by joining a downstream 3' splice donor site and an upstream 5' splice acceptor site. Several recent studies have identified circRNAs as potential biomarker for different diseases. A number of methods are available for the identification of circRNAs. The circRNA identification methods cannot provide full-length sequences. Reconstruction of the full-length sequences is crucial for the downstream analyses of circRNA research including differential expression analysis, circRNA-miRNA interaction analysis and other functional studies of the circRNAs. However, a limited number of methods are available in the literature for the reconstruction of full-length circRNA sequences. We developed a new method, circRNA-full, for full-length circRNA sequence reconstruction utilizing chimeric alignment information from the STAR aligner. To evaluate our method, we used full-length circRNA sequences produced by isocirc and ciri-long using long-reads RNA-seq data. Our method achieved better reconstruction rate, precision, sensitivity and F1 score than the existing full-length circRNA sequence reconstruction tool ciri-full for both human and mouse data.

Keywords: circular RNA; reconstruction of circRNA sequence; full-length sequence



Citation: Hossain, M.T.; Zhang, J.; Reza, M.S.; Peng, Y.; Feng, S.; Wei, Y. Reconstruction of Full-Length circRNA Sequences Using Chimeric Alignment Information. *Int. J. Mol. Sci.* **2022**, *23*, 6776. <https://doi.org/10.3390/ijms23126776>

Academic Editor: Nicholas Delihias

Received: 4 May 2022

Accepted: 13 June 2022

Published: 17 June 2022

Publisher's Note: MDPI stays neutral with regard to jurisdictional claims in published maps and institutional affiliations.



Copyright: © 2022 by the authors. Licensee MDPI, Basel, Switzerland. This article is an open access article distributed under the terms and conditions of the Creative Commons Attribution (CC BY) license (<https://creativecommons.org/licenses/by/4.0/>).

1. Introduction

Circular RNAs (circRNAs) are RNA molecules with covalently closed RNA loops, produced by joining a downstream 3' splice donor site and an upstream 5' splice acceptor site [1–3]. They are generated from both coding and noncoding linear transcripts [4]. They can comprise exonic or intronic sequences from their parent genes, and their sizes may vary from less than 100 nt to more than 4000 nt [5]. CircRNAs can originate from exons, introns, antisense, intergenic regions and 5' or 3' untranslated regions [6]. They are produced through a variety of distinct mechanisms depending on complementary sequences within flanking introns [7–9], exon skipping [9,10], and exon-containing lariat precursors [11]. Among several important properties, circRNAs have the ability to effectively sponge miRNAs [12], can interact with proteins [13] and can be translated into functional proteins [14]. CircRNAs can also interact with RNA-binding proteins (RBPs) [15], but there is minimal enrichment in RBP binding sites for circRNA sequences compared to their linear mRNA counterparts. Several studies have demonstrated that circRNA transcripts can be involved in gene regulation [16], development [17], natural immune responses [18] and diseases [19,20]. A number of studies have identified circRNAs as potential biomarkers for

cancers [21–23], autoimmune diseases [24,25], atherosclerosis [26], disorders of the central neural diseases [27], and degenerative diseases [28].

In the literature, a number of methods are available for the identification of circRNAs including *find_circ* [29], *CIRCexplorer* [8], *CIRI* [30], *circRNA_finder* [31], and *DCC* [32], among others. All of these methods identify circRNAs with their start and end position in the chromosome but cannot provide full-length circRNA sequences. The full-length sequence of the circRNA is crucial for downstream analyses in circRNA research, including differential expression analysis, circRNA-miRNA interaction analysis and other functional studies of the circRNAs. A limited number of methods, including *ciri-full* [33], *FUCHS* [34], and *FcircSEC* [35] are available for full-length circRNA sequence reconstruction. To assemble full-length circRNA sequences, *ciri-full* uses both back-splice junction (BSJ) sites and reverse overlap (RO) features. The output of *CIRI* and RNA-seq data are needed for *ciri-full* to assemble the full-length sequence. *FUCHS* is designed to fully characterize a putative circRNA sequence using RNA-seq information from long reads (>150 bp). It utilizes the internal components of the BSJ and produces the circRNA sequences using the mapping results of BSJ reads. On the other hand, *FcircSEC* is developed for the full-length circRNA sequence reconstruction and classification using the annotation information of the reference genome, and fully depends on the annotation information. Our method *circRNAfull* utilizes chimeric alignment information of the spanning reads of the circRNA. The key drawback of *ciri-full* is that it cannot be used if the sequencing read lengths for all reads in the RNA-seq data are not equal. Moreover, the annotation file in gff format is not accepted by *ciri-full*. *FUCHS* is tested with the output of *DCC* only and is not suitable for short reads, and it does not provide the full-length sequence directly. *FcircSEC* is based on annotation information of the reference genome and does not use sequencing reads. Mostly, it combines all possible exons within the circRNA boundary for exonic circRNAs. It depends on an assumption that circular and linear transcripts share the same composition. However, this assumption is unsupported and may lead to misunderstanding in downstream analyses [33]. To address these limitations, we developed a method, *circRNA-full*, for reconstructing full-length circRNA sequences utilizing the chimeric alignments of the STAR aligner.

In this paper, we present a new method, *circRNA-full*, using chimeric alignments of the STAR aligner together with the output of *CIRCexplorer*. Comparing the performance of *circRNA-full* with *ciri-full* in terms of precision, sensitivity and F1 score, we found that *circRNA-full* performed better than *ciri-full* for both human and mouse data.

2. Results

2.1. Identification of circRNAs

We identified circRNAs using two popular tools: *CIRI* (version 2) and *CIRCexplorer* (version 2). For human data, a total of 8120 circRNAs were identified by *CIRI*, whereas a total of 18,123 circRNAs were identified by *CIRCexplorer*. The number of common circRNAs identified both algorithms was 6534 (Figure 1A). A total of 13,175 circRNAs were identified by a single algorithm. Among the circRNAs identified by *CIRI*, 91.82% (7456/8120) were exonic, 8% (650/8120) were intronic and the rest were intergenic (Figure 1B). The average number of back-splice reads was five. The distribution of back-splice reads showed that 77% of the circRNAs were supported by less than or equal to four back-splice reads (Figure 1C). The chromosome distribution was heterogeneous and showed that the maximum number (831) of circRNAs were originated from chromosome 1 (Figure 1D). For the circRNAs identified by *CIRCexplorer*, there were 99.82% (18,091/18,123) exonic circRNAs and the rest were intronic. The average number of back-splice reads was two. The majority of the circRNAs (88.78%) were supported by less than or equal to two back-splice reads. The chromosome distribution was heterogeneous and the maximum number (1749) of circRNAs were originated from chromosome 1. Figure 1 showed the expression profile of circRNAs for human data.

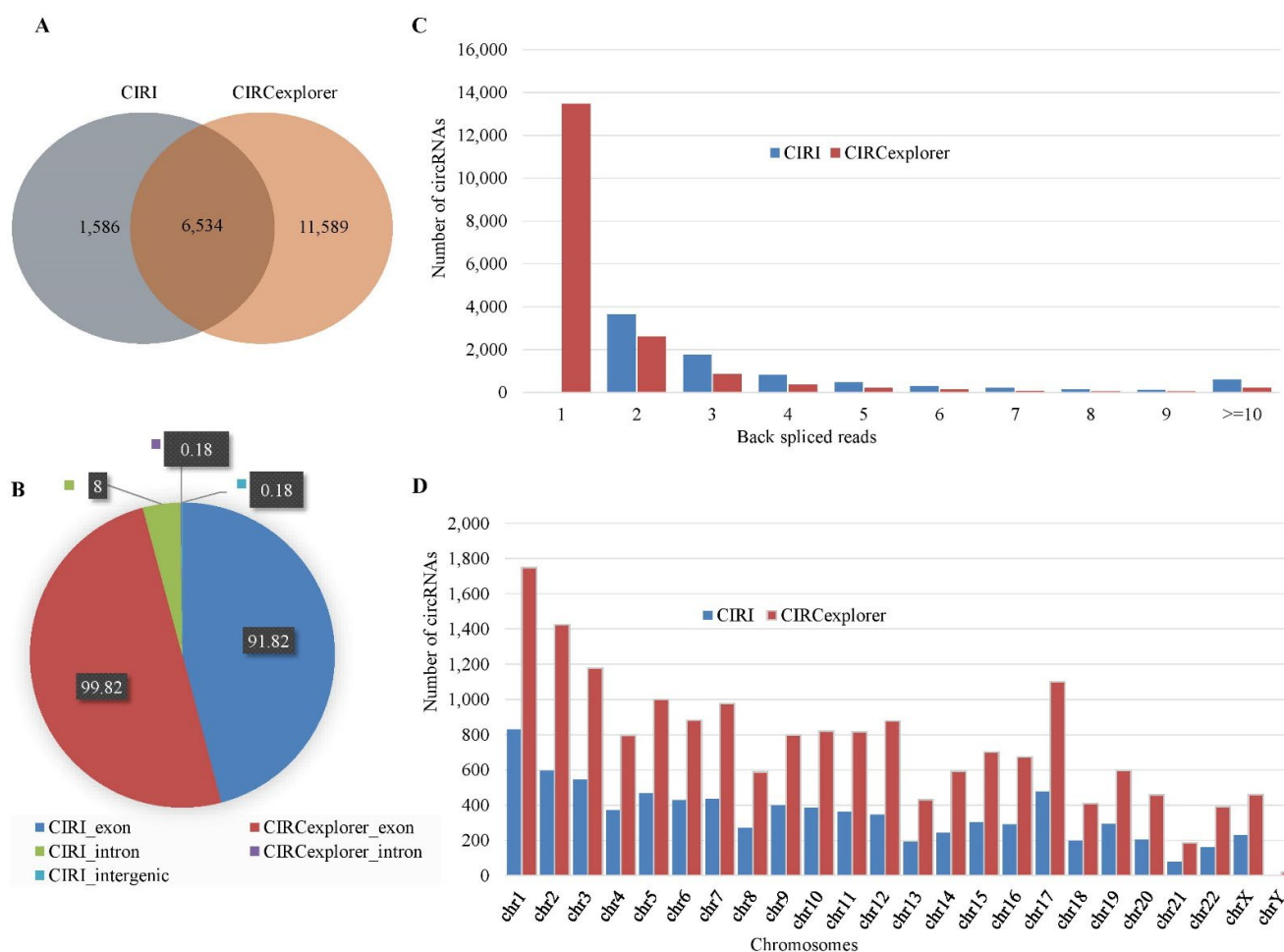


Figure 1. Expression profile of circRNAs in human data. (A) Venn-diagram of the circRNAs identified by CIRCExplorer and CIRC. (B) Distribution of the genomic origin of the circRNAs (%). (C) Distribution of the number of back-spliced reads spanning the circRNAs. (D) Chromosome distribution of the identified circRNAs.

For mouse data, 17,694 circRNAs were identified by CIRC, whereas 31,252 circRNAs were identified by CIRCExplorer. We found a total of 14,279 circRNAs were identified by both the tools, whereas 20,388 circRNAs were identified by a single method (Figure 2A). There were 90.65% (16,040/17,694) exonic, 8.23% (1456/17,694) intronic, and the rest were intergenic circRNAs among the total circRNAs identified by CIRC (Figure 2B). The average number of back-splice reads spanning the circRNAs was ten. Around 77% of the circRNAs were supported by less than or equal to seven back-splice reads. From the chromosome distribution, it was found that the distribution was heterogeneous and the maximum number of circRNAs (1513) were generated from chromosome 2 (chr2) (Figure 2D). Among the circRNAs identified by CIRCExplorer, 98% (30,756/31,252) were exonic and the rest were intronic, and no intergenic circRNAs were found. The average number of back-splice reads was four and about 81% circRNAs were spanned by less than or equal to three back-splice reads. The distribution of circRNAs in different chromosomes was heterogeneous and most circRNAs were in chromosome 2 (chr2). Figure 2 showed the expression profile of circRNAs for mouse data.

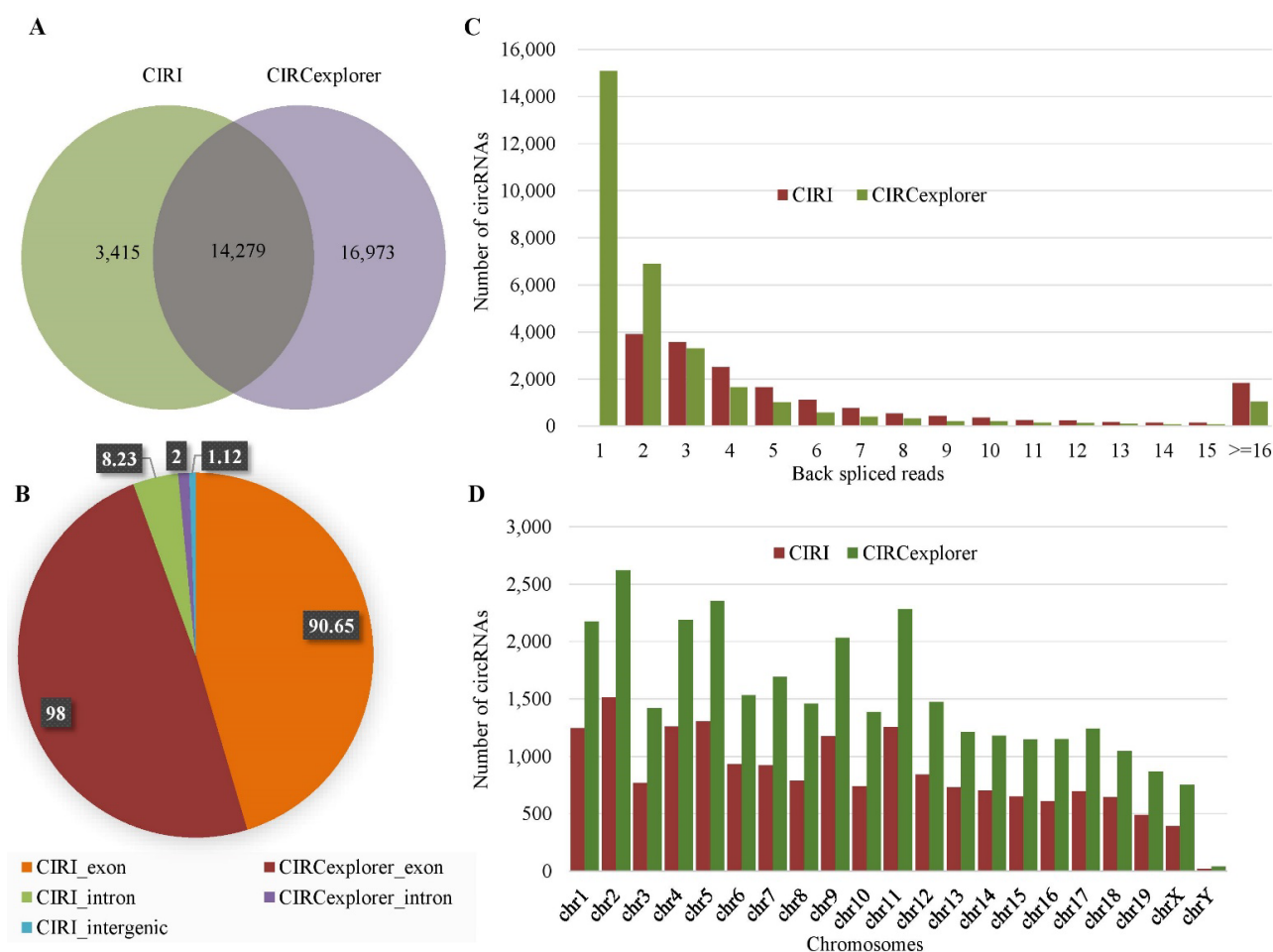


Figure 2. Expression profile of circRNAs in mouse data. (A) Venn-diagram of the circRNAs identified by CIRCexplorer and CIRCexplorer. (B) Distribution of the genomic origin of the circRNAs (%). (C) Distribution of the number of back-spliced reads spanning the circRNAs. (D) Chromosome distribution of the identified circRNAs.

We found that more circRNAs were predicted by CIRCexplorer than CIRCexplorer in human and mouse data. No circRNAs identified by CIRCexplorer were spanned by less than two back-spliced reads, whereas 74% and 48% of the circRNAs identified by CIRCexplorer were spanned by only one back-splice read in human and mouse data respectively. Moreover, the circRNAs produced by CIRCexplorer were supported by larger average number of back-splice reads than that of the circRNAs produced by CIRCexplorer in both datasets. More circRNAs were identified in mouse than human, and the average number of back-splice reads per circRNA was larger in mouse than human.

2.2. Reconstruction of Full-Length Sequence

We reconstructed full-length sequences of the circRNAs using the circRNA-full and our developed method circRNA-full. We used two tools, CIRCexplorer and CIRCexplorer, for the prediction of circRNAs. For reconstructing the full-length sequence, we used those circRNAs which were identified by both CIRCexplorer and CIRCexplorer. The reason was to use the same set of circRNAs for the performance comparison of circRNA-full and circRNA-full.

For human data, a total of 5130 full-length circRNAs were assembled by circRNA-full, whereas 5737 full-length circRNAs were assembled by our method, circRNA-full. Among these full-length circRNAs, 75.56% of the circRNAs were assembled by both circRNA-full and circRNA-full, whereas 7.32% of the circRNAs were assembled by circRNA-full only, and 17.12% of the circRNAs were assembled by circRNA-full only (Figure 3A). For mouse

data, 12,711 full-length circRNAs were assembled by ciri-full, whereas 13,998 full-length circRNAs were assembled by circRNA-full. Moreover, 90.03% of the circRNAs were assembled by both ciri-full and circRNA-full (Figure 3B). Of the circRNAs, 0.41% and 9.56% were assembled by the single assembly methods ciri-full and circRNA-full, respectively (Figure 3B). More full-length circRNAs were assembled in mouse than human.

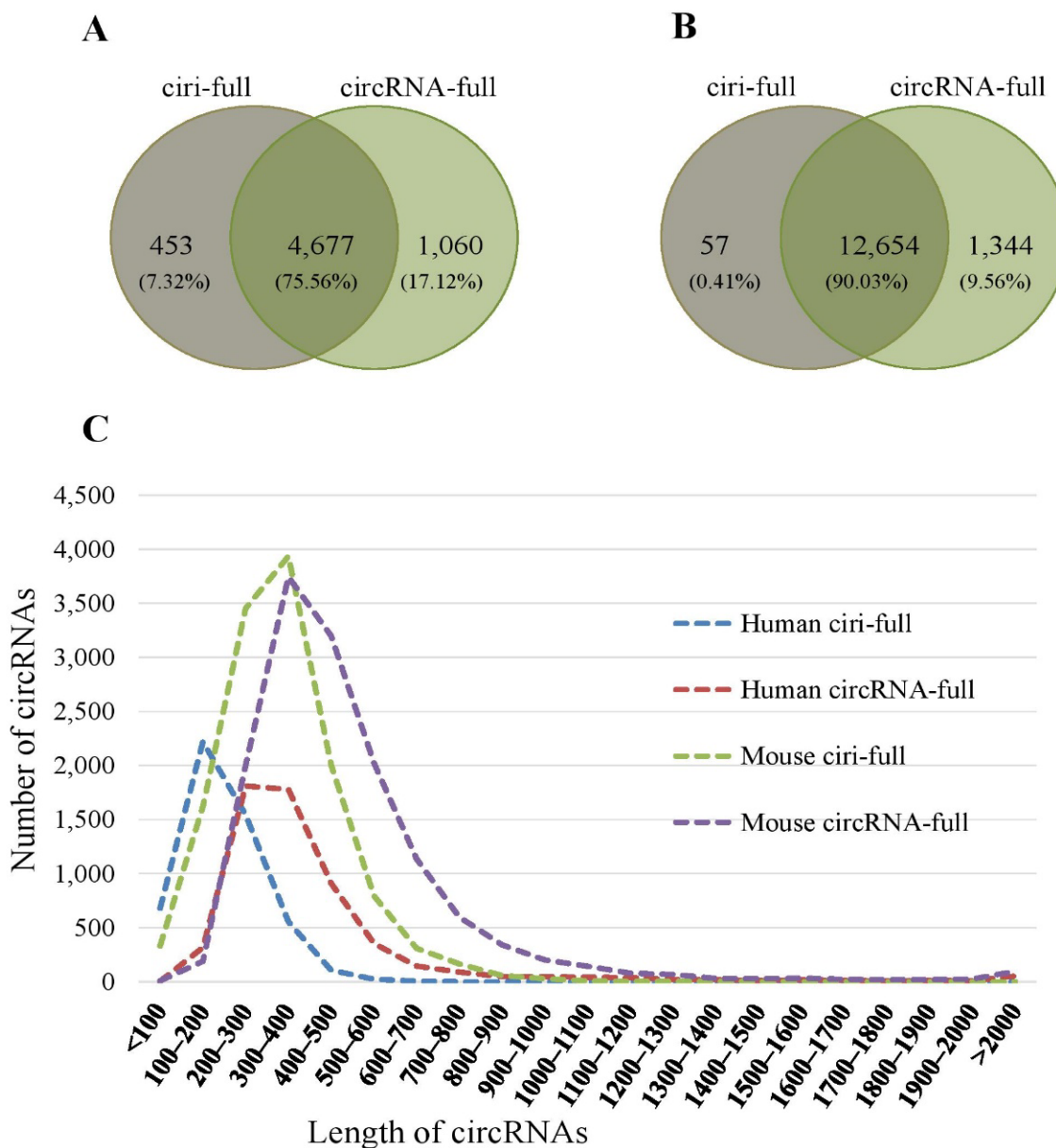


Figure 3. Sequence reconstruction results for circRNA-full and ciri-full. (A) Venn-diagram of the number of reconstructed circRNAs for human data. (B) Venn-diagram of the number of reconstructed circRNAs for the mouse data. (C) Length distribution of reconstructed circRNAs.

From Table 1, it can be observed that the assembly rate of circRNA-full was more than that of the ciri-full. For sample SRR10612068, 81.15% of the circRNAs were assembled by ciri-full, whereas 90.81% of the circRNAs were assembled by circRNA-full. For mouse data, in sample CRR194214, 94.95% of the circRNAs were reconstructed by ciri-full, whereas 99.58% of the circRNAs were reconstructed by circRNA-full. Between human and mouse data, the percentage of assembled sequences was more in the mouse data. From Figure 3C, we can observe that the length of most of the circRNAs were less than 1000 nt. The length of the circRNAs reconstructed by circRNA-full was longer than that of the circRNAs produced

by *ciri-full* in both human and mouse data. Again, the length of the circRNAs in mouse data was longer than that of the circRNAs in human data.

Table 1. Number of reconstructed sequences produced by *ciri-full* and *circRNA-full* for different samples.

Species	Sample	NSC	<i>ciri-Full</i>		<i>circRNA-Full</i>	
			NRS	% of RS	NRS	% of RS
<i>Homo Sapiens</i>	SRR10612068	3756	3048	81.15	3411	90.81
	SRR10612069	3254	2552	78.43	2959	90.93
	SRR10612070	3290	2616	79.51	3002	91.25
<i>Mus Musculus</i>	CRR194214	9699	9209	94.95	9658	99.58
	CRR194215	10,911	8649	79.27	10,864	99.57

Note: NSC = Number of sequences used for comparison, NRS = Number of reconstructed sequences, RS = Reconstructed sequences.

For human data, it was found that the length of circRNAs produced by *circRNA-full* (median 334) was greater than that of the circRNAs produced by *ciri-full* (median 182), and the number was statistically significant as determined by the Mann-Whitney U-test ($p < 2.20 \times 10^{-16}$). We also observed that 75% of the circRNAs had a length of 432 nt for *circRNA-full* and of 250 nt for *ciri-full*. For mouse data, the length of circRNAs produced by *circRNA-full* (median 428) was greater than that of the circRNAs produced by *ciri-full* (median 320) with $p < 2.20 \times 10^{-16}$ determined by the Mann-Whitney U-test. Again 75% of the circRNAs had a length of 559 nt for *circRNA-full* and of 406 nt for *ciri-full*. For combined data (human and mouse) the length of circRNAs generated by *circRNA-full* (median 400) was greater than that of the circRNAs generated by *ciri-full* (median 283), which was significant as determined by Mann-Whitney U-test ($p < 2.20 \times 10^{-16}$). Seventy-five percent of the circRNAs had lengths of less than 529 nt for *circRNA-full* and less than 372 nt for *ciri-full*.

2.3. Performance Comparison of *ciri-Full* and *circRNA-Full*

Full-length circRNA sequences of the existing databases were constructed using a combination of all exons within the back-spliced junction sites. So far, there are no databases for the full-length sequences of experimentally validated circRNAs. There are two tools, *isocirc* and *ciri-long*, which both have a computational pipeline to reliably characterize full-length circRNA isoforms using long-read RNA sequencing data. The full-length circRNA sequences produced by *isocirc* and *ciri-long* were used as the validated full-length circRNA resources to compare our developed method, *circRNA-full*, with *ciri-full*.

We reconstructed full-length sequences using *ciri-full* and our method, *circRNA-full*. We used *isocirc* for human data and *ciri-long* for mouse data to obtain validated full-length circRNA resources, as the length of the long reads for human data was greater than 1000 bp and for mouse data the length of the long reads was less than 1000 bp. We determined the sequence to be correctly reconstructed if the sequence identified by *ciri-full* or *circRNA-full* was identical with the sequences identified by *isocirc* or *ciri-long*.

We used three accuracy measurements: precision, sensitivity and F1 score to compare the performance of *ciri-full* and *circRNA-full*. The precisions of *circRNA-full* (56.93, 57.69, and 58.93%) were higher than that of *ciri-full* (40.85, 40.52, and 41.28%) for the three samples in human data (Table 2). Again, the precisions of *circRNA-full* (22.14% and 21.31%) were higher than that of *ciri-full* (21.34% and 20.79%) for the two samples in mouse data. *circRNA-full* achieved higher sensitivity (95.15, 94.89, and 94.95%) than *ciri-full* (79.35, 74.66, and 76.60%) for the three samples in human data. In the mouse data, *circRNA-full* also achieved higher sensitivity (99.67 and 99.78%) than *ciri-full* (97.47 and 81.06%). The F1 scores of *circRNA-full* (0.7124, 0.7175, and 0.7272) were higher than that of *ciri-full* (0.5393, 0.5253, and 0.5365) for three samples in human data. Again, *circRNA-full* gained higher F1 scores (0.3623 and 0.3512) than *ciri-full* (0.3501 and 0.3309) for two samples in mouse data.

Table 2. Performance comparison of circRNA-full and circRNA-full using different accuracy measures.

Species	Sample	Method	NRS	TP	FN	Precision	Sensitivity	F1 Score
<i>Homo sapiens</i>	SRR10612068	circRNA-full	3048	1245	324	40.85%	79.35%	0.5393
		circRNA-full	3411	1942	99	56.93%	95.15%	0.7124
	SRR10612069	circRNA-full	2552	1034	351	40.52%	74.66%	0.5253
		circRNA-full	2959	1707	92	57.69%	94.89%	0.7175
	SRR10612070	circRNA-full	2616	1080	330	41.28%	76.60%	0.5365
		circRNA-full	3002	1769	94	58.93%	94.95%	0.7272
<i>Mus Musculus</i>	CRR194214	circRNA-full	9209	1965	51	21.34%	97.47%	0.3501
		circRNA-full	9658	2138	7	22.14%	99.67%	0.3623
	CRR194215	circRNA-full	8649	1798	420	20.79%	81.06%	0.3309
		circRNA-full	10864	2315	5	21.31%	99.78%	0.3512

Note: NRS = Number of reconstructed sequences, TP = True positives, FN = False negatives.

The reconstruction rate of circRNA-full was greater than that of circRNA-full for human and mouse data (Figure 4A). The precision of circRNA-full was higher than that of circRNA-full for all samples (Figure 4B). CircRNA-full achieved greater sensitivity than circRNA-full for both the data sets (Figure 4C). CircRNA-full gained larger F1 score than that of circRNA-full for all samples (Figure 4D). Overall, we found that our developed method, circRNA-full, showed better performance than circRNA-full.

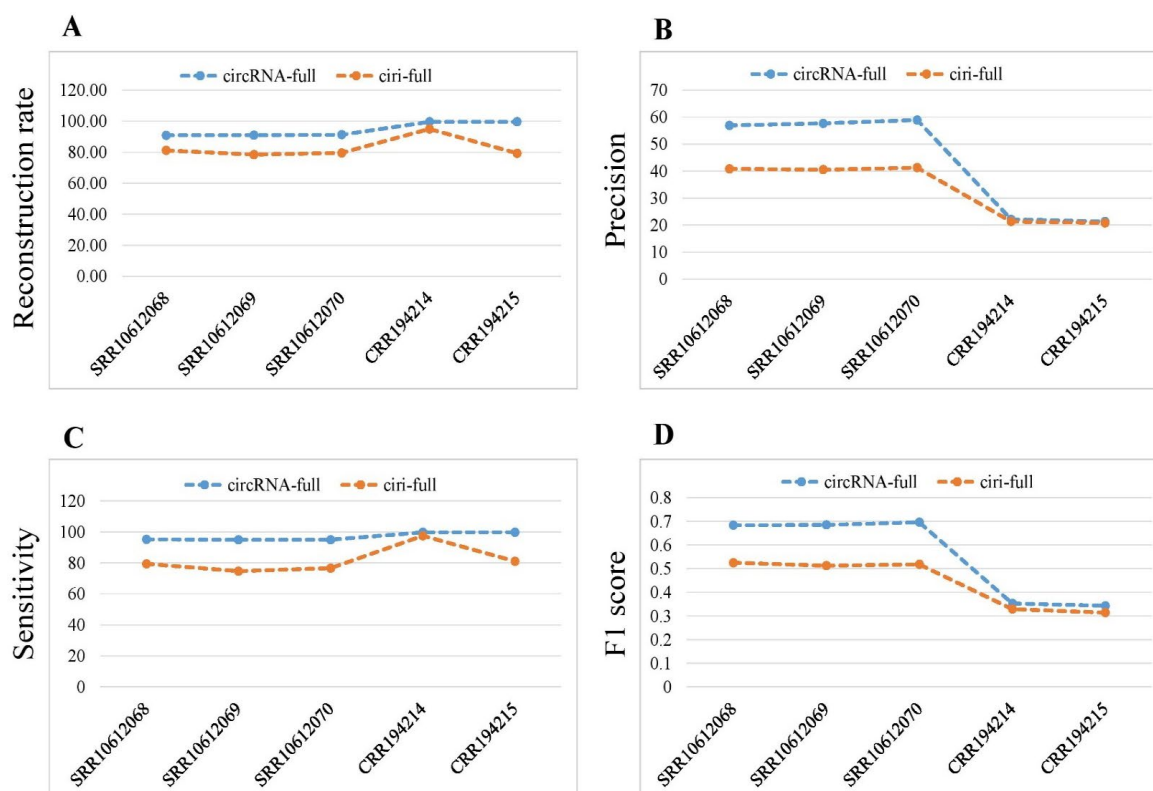


Figure 4. Performance comparison of circRNA-full and circRNA-full. (A) Reconstruction rate. (B) Precision. (C) Sensitivity. (D) F1 score for different samples.

3. Discussion

There are several circRNA prediction tools, but a limited number of methods to reconstruct full-length circRNA sequences. Full-length circRNA sequence reconstruction is crucial to explore the functions of circRNA. We developed a new method, circRNA-full, for the reconstruction of full-length circRNA sequences utilizing the chimeric alignment information from STAR aligner. We validated our method with the reliable full-length circRNAs generated by isocirc and circRNA-long from the long reads RNA sequencing data.

We reconstructed full-length sequences by our method, circRNA-full, and using *ciri-full* for human and mouse data. We found that circRNA-full reconstructed more full-length circRNA sequences (in percentage) compared to *ciri-full*. More full-length circRNAs were produced in mouse data than human as the read lengths of mouse data were longer than human. CircRNA-full produced longer full-length circRNA sequences compared to *ciri-full* in both human and mouse data. The number of back-spliced reads was greater in mouse data than in human data for the full-length circRNA reconstructed by both circRNA-full and *ciri-full*.

For full-length circRNA sequence reconstruction, a limited number of approaches are available, including *ciri-full*, FUCHS, and FcircSEC. *Ciri-full* uses both BSJ (back-splice junction) sites and RO (reverse overlap) properties and require sequencing data to assemble full-length circRNA sequences. The main drawback of *ciri-full* is that it is not applicable if the sequencing read lengths for all reads in the RNA-seq data are not equal. FUCHS characterizes putative full-length circRNA sequences using RNA-seq information from long reads (>150 bp). It is not suitable for short reads and doesn't provide the full-length sequence directly. FcircSEC is designed for full-length circRNA sequence reconstruction and classification using the annotation information of the reference genome. It depends fully on annotation information, and sequence information is not utilized in this method. Our developed method circRNA-full is free from the limitations mentioned in the existing methods.

We compared the performance of circRNA-full and *ciri-full* based on precision, sensitivity and F1 score. The reconstruction rate of circRNA-full was higher than *ciri-full* in both human and mouse data. CircRNA-full achieved higher precision, sensitivity and F1 score than *ciri-full* in both human and mouse data. Thus, we can conclude that our developed method, circRNA-full, performed better than *ciri-full*.

We evaluated our method by comparing the sequences produced by our method with the sequences produced by *isocirc/ciri-long*. We assume that the sequences produced by *isocirc* and *ciri-long* are correct. The methods *isocirc* and *ciri-long* utilize long reads RNA-seq data; these data are relatively low throughput and the error rate of long read sequencing technology is relatively high. Therefore, *isocirc* and *ciri-long* may produce incorrect sequences sometimes, which may affect slightly the evaluation metrics of our method. This issue does not affect the performances of our method much because the evaluation metrics of our method are relatively high compared to the existing method, *ciri-full*.

4. Materials and Methods

Our method, circRNA-full, requires five types of input: (1) the output of the circRNA prediction tool CIRCexplorer, (2) chimeric alignments (in bam) produced by STAR, (3) chimeric junction (junction file) generated by STAR, (4) a reference genome, and (5) annotation of the reference genome. For each circRNAs, we extracted the individual alignments of the spanning reads of the circRNA. From the individual alignments, we extracted exons and introns utilizing the CIGAR value of the alignments. Then, we detected skip exons (if any) defined as the intersection part between exons and introns. Finally, the skip exons were deleted from the exons set and the remaining exons composed the full-length sequence. We compared the performance of our method, circRNA-full, with the existing method *ciri-full* based on precision, sensitivity and F1 score. As there is no resources/databases for the experimentally validated circRNAs, we used two tools, *isocirc* [5] and *ciri-long* [36], to build comparatively reliable validated circRNA resources to compare our method. Both of these tools, *isocirc* and *ciri-long*, are computational pipelines to reliably characterize full-length circRNA isoforms using long-read RNA sequencing data. We defined a sequence reconstructed by *ciri-full/circRNA-full* as correct if it was identical with the sequences identified by *isocirc* or *ciri-long*.

4.1. Data Description

The short reads NGS (next generation sequencing) RNA-seq data were downloaded from the Sequence Reads Archive (accession number: SRR10612068, SRR10612069, SRR10612070) and the National Genomics Data Center (<https://bigd.big.ac.cn/gsa>, accessed on 3 November 2021) (accession number: CRR194214, CRR194215). Long reads third generation sequencing (Nanopore sequencing) data were downloaded from the Sequence Reads Archive (accession number: SRR10612050, SRR10612051, SRR10612052, SRR10612053, SRR10612054, and SRR10612055) and the National Genomics Data Center (accession number: CRR194190, CRR194191, CRR194194, and CRR194195). Both the short reads and long reads downloaded from the same database were derived from same experiment samples. All the sequencing data downloaded from Sequence Reads Archive were derived from the cultured HEK293 cells, and all the data downloaded from the National Genomics Data Center were derived from adult mice. The reference genomes of human (GRCh38/hg38) and mouse (GRCm39/mm39) were downloaded from UCSC.

To evaluate the performance of our method, we compared the sequences produced by our method with experimentally validated circRNA sequences. In the literature there are no databases/resources for experimentally validated circRNA sequences, but there are two tools, isocirc and ciri-long, which can reliably characterize full-length circRNA isoforms using long-read RNA sequencing data. The limitations of long reads third generation sequencing data are that the error rate of these data are relatively high, and they are relatively low throughput. Despite having these limitations, we used long reads third generation data to obtain comparatively reliable full-length circRNA sequences.

4.2. Extract Alignments of Spanning Reads for Individual circRNA

In this step, we extracted the alignments of spanning reads for each circRNA using the output of CIRCexplorer and the chimeric alignment bam file produced by STAR. The circRNAs were produced by some spanning reads and in this step we extracted the alignment results of these spanning reads for each individual circRNA.

The inputs of this step were: (1) the list of all circRNAs with the name of their spanning reads, and (2) the alignment bam file containing all chimeric reads. Input 1 was a two-column txt file where the first column contained chromosome, start and end position of circRNAs separated by ":" and "|". The second column contained the list of spanning reads of the circRNAs separated by commas. Input 2 was the standard alignment bam file containing only the chimeric reads. The output of this step generated a separate txt file for each circRNA that contained the alignment of chimeric reads that spanned that circRNA. The pictorial representation of this step was given in Figure 5.

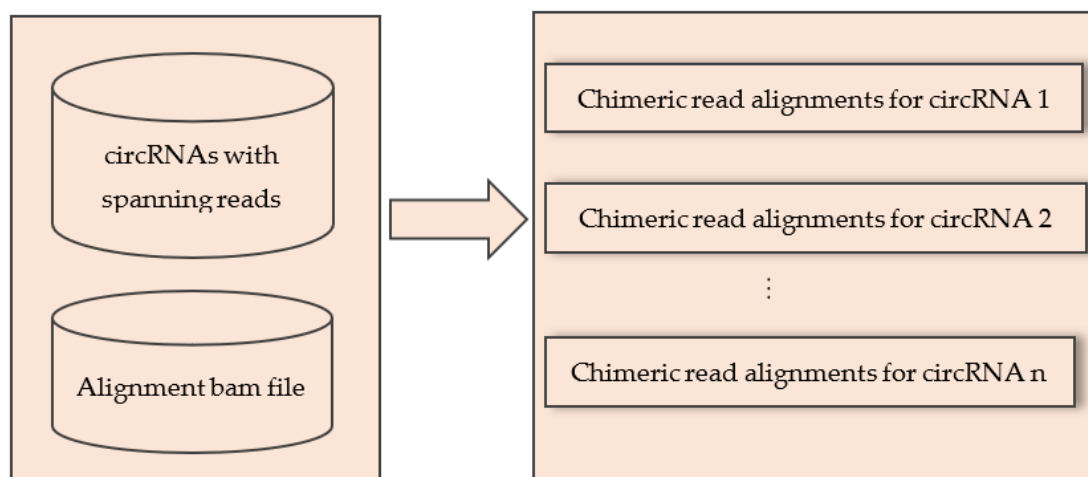


Figure 5. Extracting alignment of circRNA spanning reads for each circRNA from the alignment bam file.

4.3. Extract Exons/Introns from the CIGAR Value of Bam File

In this step, we extracted exons from the CIGAR value of the chimeric read alignment bam file. We utilized the CIGAR string M and N to extract exons and introns, respectively, where M represented matches in exons and N represented skip elements due to introns. For example, if the alignment start position at $POS = 125314967$ and $CIGAR = 67M8354N57M7713N81M44S$, then the procedure of extracting exons/introns was as follows. Let us define,

$$s_i = \begin{cases} POS & \text{for } i = 1 \\ e_{i-1} + 1 & \text{for } i = 2, 3, \dots \end{cases} \quad e_i = s_i + n_i - 1 \text{ for } i = 1, 2, \dots$$

where n_i is the number corresponding to CIGAR string, s_i is the start position and e_i is the end position of the corresponding exon or intron.

In Table 3, M represents the exons and columns 6 and 7 show the corresponding exon start and end positions. On the other hand, N represents introns and columns 3 and 4 show the corresponding intron start and end positions. The CIGAR value also contained the characters such as S, H, D, and I. However, we were not interested in these characters and they had no effect on our method. Extraction of exons was not fully dependent on CIGAR string. The exons obtained from CIGAR string were compared with exons in the gene annotation information. If any exon obtained from CIGAR string intersected with an exon in the reference genome annotation, the exon from annotation was selected as final exon.

Table 3. Process of extracting exons and introns from the CIGAR value of chimeric alignments.

CIGAR String	Corresponding Number n_i	Start $s_i=e_{i-1}+1$	End $e_i=s_i+n_i-1$	Transcript Name	Intersecting Exon Start	Intersecting Exon End
M	67	125314967	125315033	NM_021964	125313307	125313656
N	8354	125315034	125323387			
M	57	125323388	125323444	NM_021964	125323308	125323444
N	7713	125323445	125331157			
M	81	125331158	125331238	NM_021964	125331157	125331238

The inputs of this step were: (1) alignments of chimeric reads for each circRNA and (2) the annotation file (corresponding to reference genome). The CIGAR value of the chimeric read was used to extract the exons. Input 1 was a 13 column txt file containing the alignment information (alignment start position, cigar value etc.). Input 2 contained the coordinate of each exon from the annotation file. Input 1 contained the alignment start position for each chimeric read, and the alignment end position was obtained using the CIGAR information. Then, from input 2, the exons having some intersection with the alignment start and end position of CIGAR string M of the chimeric read were selected as final exons set. Figure 6 is a pictorial representation of this step.

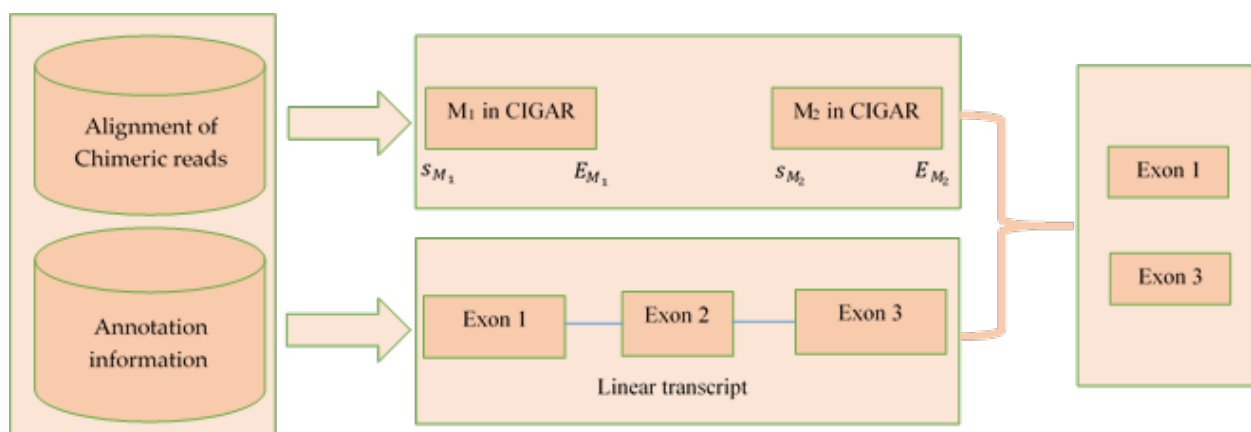


Figure 6. Procedure of extracting exons from the CIGAR string from the alignment of chimeric read.

4.4. Detecting Skip Exons

The procedure of extracting exons/introns from the CIGAR string is described in Table 3 in Section 4.3. After obtaining the introns, we investigated whether there was any intersection between the introns and the exons. If we found any intersection between exons and introns, we defined the intersection part as a skip exon. A full exon or a part of an exon might be detected as a skip exon. The detailed procedure is shown in Figure 7.

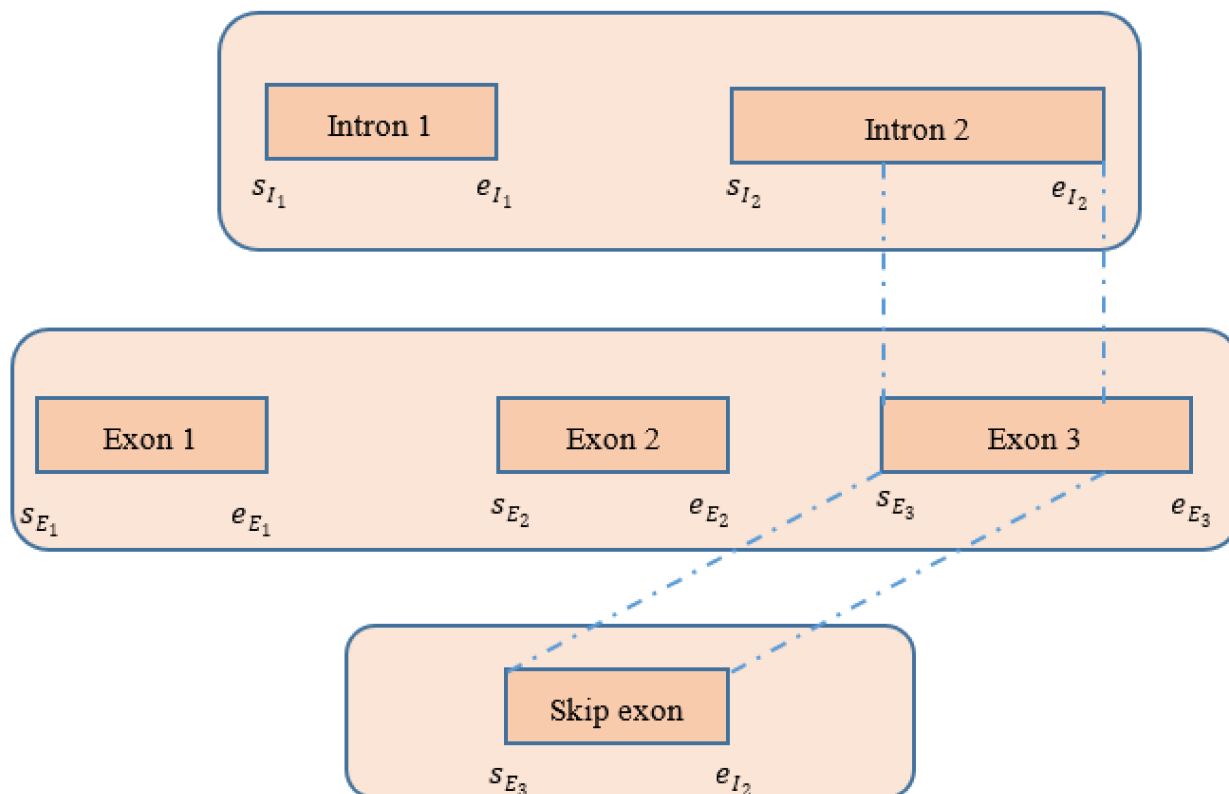


Figure 7. Procedure of detecting skip exon after extracting exons and introns from the CIGAR string of the spanning chimeric reads.

4.5. Deletion of Skip Exon and Reconstruction of Full Sequence

We extracted the exons and introns utilizing the CIGAR value of the chimeric alignments of the spanning reads of the circRNA. Then, we detected the skip exon (if any) as the intersection part of exon and intron. In this step, we deleted the skip exon from the available exons and obtained the final exons set. Finally, combining these exons sets, we reconstructed the full-length sequence of circRNAs. The detailed procedure is shown in Figure 8.

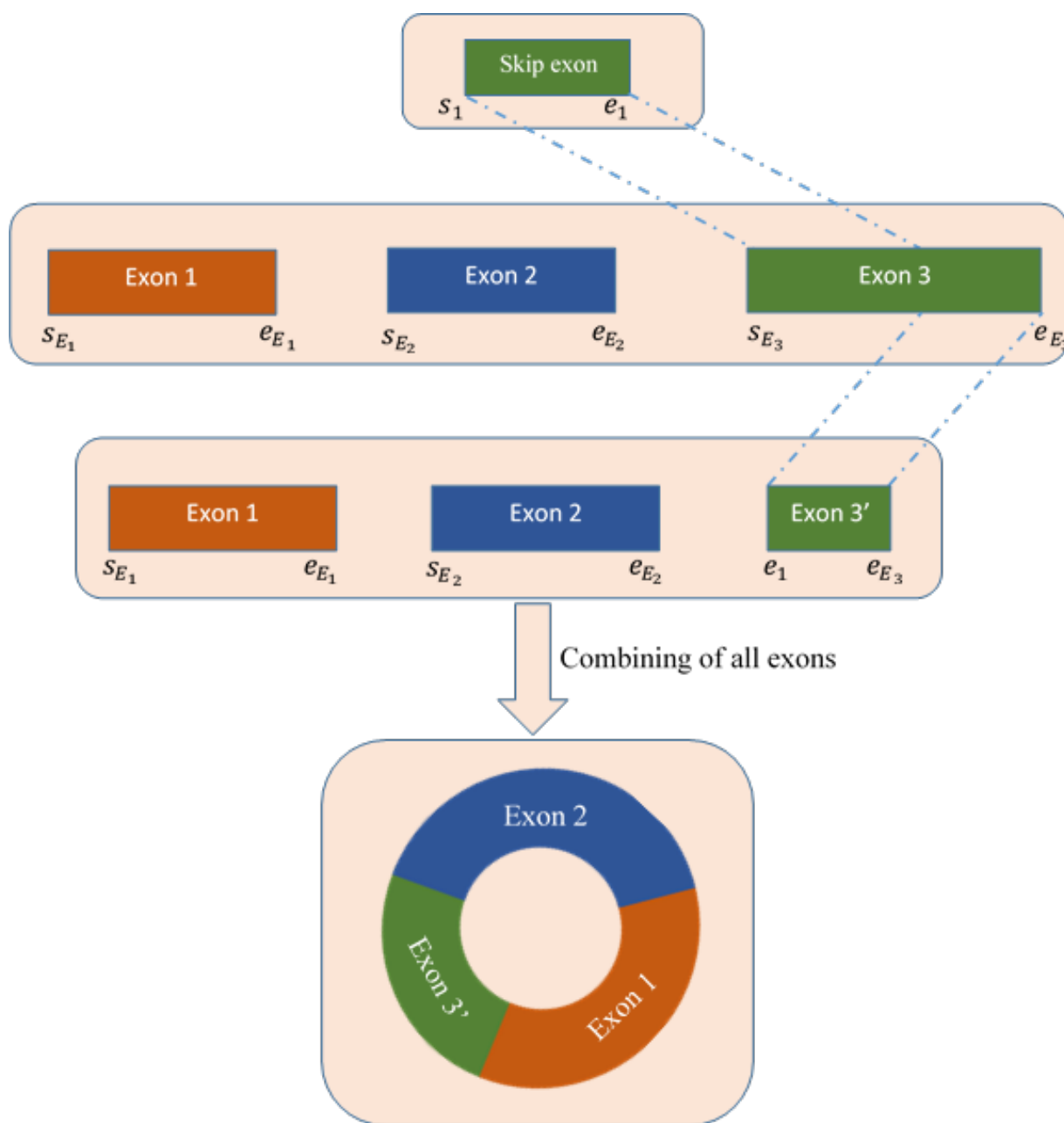


Figure 8. Procedure of deleting skip exon from all available exons extracted from the CIGAR string of the spanning chimeric reads.

4.6. Identification of circRNAs and Reconstruction of Full-Length Sequences

We used two popular circRNA prediction tools, CIRI (version 2) and CIRCexplorer (version 2), for the identification of circRNA. For mapping the sequencing reads to the genome, we used BWA [37] for CIRI, and STAR [38] for CIRCexplorer with default parameters. For the reconstruction of full-length circRNA sequences, we used ciri-full and our developed method, circRNA-full. Both of these two methods required information of identified circRNAs and sequencing reads as input.

4.7. Evaluation Criteria for Performance Comparison

We reconstructed full-length circRNA sequences using long-reads (produced by Nanopore technology) as validated circRNA sequences because no databases for experimentally validated circRNAs are available in the literature. We assessed the reconstructed

sequences produced by short reads compared with the sequences produced by long reads, provided that both the short reads and long reads were derived from the same sample.

So far, in the literature, two tools isocirc and ciri-long, are available for reconstructing full-length circRNA sequences using long reads. These tools are used to reliably characterize full-length circRNA isoforms using long-read RNA sequencing data. A sequence reconstructed by short reads was considered correct if it was similar to any one of the sequences produced by isocirc. Similarly, a reconstructed sequence produced by short reads was declared correct if it was similar to any of the sequences produced by ciri-long. The similarity of the sequences produced by short reads and long reads was defined according to criteria 1 and 2.

criteria 1. A and B have more than 95% similarity

criteria 2. $|M - \text{average}\{l(A), l(B)\}| < 10$

where A and B are the sequences produced by short reads and long reads, respectively, M is the number of matched elements between A and B , and $l(A)$ and $l(B)$ are the length of A and B respectively.

The reconstructed full-length circRNA sequences verified by long reads were defined as true positives, whereas those not verified by long reads were defined as false positives. The full-length circRNA sequences that were verified by long reads in other reconstruction method (e.g., ciri-full) but not assembled in current reconstruction method (e.g., circRNA-full) were defined as false negatives in the current reconstruction method. The evaluation metrics used for comparing the performance of circRNA-full with ciri-full are defined as follows:

$$\text{Precision} = \frac{TP}{TP + FP}$$

$$\text{Sensitivity} = \frac{TP}{TP + FN}$$

$$\text{F1 Score} = \frac{2 * \text{precision} * \text{sensitivity}}{\text{precision} + \text{sensitivity}}$$

where TP , FP and FN are the number of true positives, false positives and false negatives, respectively.

5. Conclusions

Several methods are available in the literature for the identification of circRNAs. However, a limited number of methods are available for the reconstruction of full-length circRNA sequences. We developed a new method, circRNA-full, for full-length circRNA sequence reconstruction incorporating chimeric alignment information. We evaluated the performance of our method with full-length circRNA sequences produced by isocirc and ciri-long using long-reads RNA-seq data. Our method, circRNA-full, had a better reconstruction rate, precision, sensitivity and F1 score than the existing full-length circRNA sequence reconstruction tool, ciri-full, for both human and mouse data. We developed an R package for our method which is freely available at <https://github.com/tofazzalh/circRNAFull>.

Author Contributions: M.T.H. and Y.P. and Y.W. designed the study. M.T.H. performed the bioinformatics pipelines, analyzed the data, wrote the manuscript and drew the figures and tables. J.Z., M.S.R., Y.P., S.F. and Y.W. extensively edited the manuscript. S.F. and Y.W. supervised the work. All the authors read and approved the final version of the manuscript for publication. All authors have read and agreed to the published version of the manuscript.

Funding: This work was partly supported by the National Key Research and Development Program of China under Grant No. 2018YFB0204403, key Research and Development Project of Guangdong Province under grant no. 2021B0101310002, Strategic Priority CAS Project XDB38050100, National Science Foundation of China under grant no. U1813203, the Shenzhen Basic Research Fund under grant no RCYX2020071411473419, KQTD20200820113106007 and JSJG20201102163800001, CAS Key Lab under grant no. 2011DP173015. We would also like to thank funding support by the Youth Innovation Promotion Association (Y2021101), CAS to Yanjie Wei.

Institutional Review Board Statement: Not applicable.

Informed Consent Statement: Not applicable.

Data Availability Statement: Not applicable.

Acknowledgments: We would like to thank all the members of Computational Biology and Bioinformatics Lab, Center for High Performance Computing, SIAT, CAS for their valuable suggestions and feedbacks.

Conflicts of Interest: The authors declare no conflict of interest. The funders had no role in the design of the study; in the collection, analyses, or interpretation of data; in the writing of the manuscript, or in the decision to publish the results.

References

1. Li, L.; Zheng, Y.-C.; Kayani, M.U.R.; Xu, W.; Wang, G.-Q.; Sun, P.; Hai-Tao, Z.; Zhang, L.-N.; Guan-Qun, W.; Wu, L.-C.; et al. Comprehensive analysis of circRNA expression profiles in humans by RAISE. *Int. J. Oncol.* **2017**, *51*, 1625–1638. [[CrossRef](#)] [[PubMed](#)]
2. Kristensen, L.S.; Andersen, M.S.; Stagsted, L.V.W.; Ebbesen, K.K.; Hansen, T.B.; Kjems, J. The biogenesis, biology and characterization of circular RNAs. *Nat. Rev. Genet.* **2019**, *20*, 675–691. [[CrossRef](#)] [[PubMed](#)]
3. Li, X.; Yang, L.; Chen, L.L. The Biogenesis, Functions, and Challenges of Circular RNAs. *Mol. Cell* **2018**, *71*, 428–442. [[CrossRef](#)] [[PubMed](#)]
4. Rahimi, K.; Venø, M.T.; Dupont, D.M.; Kjems, J. Nanopore sequencing of brain-derived full-length circRNAs reveals circRNA-specific exon usage, intron retention and microexons. *Nat. Commun.* **2021**, *12*, 4825. [[CrossRef](#)] [[PubMed](#)]
5. Xin, R.; Gao, Y.; Gao, Y.; Wang, R.; Kadash-Edmondson, K.E.; Liu, B.; Wang, Y.; Lin, L.; Xing, Y. isoCirc catalogs full-length circular RNA isoforms in human transcriptomes. *Nat. Commun.* **2021**, *12*, 266. [[CrossRef](#)] [[PubMed](#)]
6. Salzman, J.; Gawad, C.; Wang, P.L.; Lacayo, N.; Brown, P.O. Circular RNAs are the predominant transcript isoform from hundreds of human genes in diverse cell types. *PLoS ONE* **2012**, *7*, e30733. [[CrossRef](#)] [[PubMed](#)]
7. Jeck, W.R.; Sorrentino, J.A.; Wang, K.; Slevin, M.K.; Burd, C.E.; Liu, J.; Marzluff, W.F.; Sharpless, N.E. Circular RNAs are abundant, conserved, and associated with ALU repeats. *RNA* **2013**, *19*, 141–157. [[CrossRef](#)]
8. Zhang, X.O.; Wang, H.B.; Zhang, Y.; Lu, X.; Chen, L.L.; Yang, L. Complementary sequence-mediated exon circularization. *Cell* **2014**, *159*, 134–147. [[CrossRef](#)]
9. Ivanov, A.; Memczak, S.; Wyler, E.; Torti, F.; Porath, H.T.; Orejuela, M.R.; Piechotta, M.; Levanon, E.Y.; Landthaler, M.; Dieterich, C.; et al. Analysis of intron sequences reveals hallmarks of circular RNA biogenesis in animals. *Cell Rep.* **2015**, *10*, 170–177. [[CrossRef](#)]
10. Kelly, S.; Greenman, C.; Cook, P.R.; Papantonis, A. Exon Skipping Is Correlated with Exon Circularization. *J. Mol. Biol.* **2015**, *427*, 2414–2417. [[CrossRef](#)]
11. Barrett, S.P.; Wang, P.L.; Salzman, J. Circular RNA biogenesis can proceed through an exon-containing lariat precursor. *eLife* **2015**, *4*, e07540. [[CrossRef](#)] [[PubMed](#)]
12. Hansen, T.B.; Jensen, T.I.; Clausen, B.H.; Bramsen, J.B.; Finsen, B.; Damgaard, C.K.; Kjems, J. Natural RNA circles function as efficient microRNA sponges. *Nature* **2013**, *495*, 384–388. [[CrossRef](#)] [[PubMed](#)]
13. Abdelmohsen, K.; Panda, A.C.; Munk, R.; Grammatikakis, I.; Dudekula, D.B.; De, S.; Kim, J.; Noh, J.H.; Kim, K.M.; Martindale, J.L.; et al. Identification of HuR target circular RNAs uncovers suppression of PABPN1 translation by CircPABPN1. *RNA Biol.* **2017**, *14*, 361–369. [[CrossRef](#)] [[PubMed](#)]
14. Legnini, I.; Di Timoteo, G.; Rossi, F.; Morlando, M.; Briganti, F.; Sthandier, O.; Fatica, A.; Santini, T.; Andronache, A.; Wade, M.; et al. Circ-ZNF609 Is a Circular RNA that Can Be Translated and Functions in Myogenesis. *Mol. Cell* **2017**, *66*, 22–37.e9. [[CrossRef](#)]
15. Hentze, M.W.; Preiss, T. Circular RNAs: Splicing's enigma variations. *EMBO J.* **2013**, *32*, 923–925. [[CrossRef](#)]
16. Chen, Y.G.; Satpathy, A.T.; Chang, H.Y. Gene regulation in the immune system by long noncoding RNAs. *Nat. Immunol.* **2017**, *18*, 962–972. [[CrossRef](#)]
17. Kristensen, L.S.; Hansen, T.B.; Venø, M.T.; Kjems, J. Circular RNAs in cancer: Opportunities and challenges in the field. *Oncogene* **2018**, *37*, 555–565. [[CrossRef](#)]

18. Li, X.; Liu, C.X.; Xue, W.; Zhang, Y.; Jiang, S.; Yin, Q.F.; Wei, J.; Yao, R.W.; Yang, L.; Chen, L.L. Coordinated circRNA Biogenesis and Function with NF90/NF110 in Viral Infection. *Mol. Cell* **2017**, *67*, 214–227.e7. [[CrossRef](#)]
19. Hirsch, S.; Blätte, T.J.; Grasedieck, S.; Cocciardi, S.; Rouhi, A.; Jongen-Lavrencic, M.; Paschka, P.; Krönke, J.; Gaidzik, V.I.; Döhner, H.; et al. Circular RNAs of the nucleophosmin (NPM1) gene in acute myeloid leukemia. *Haematologica* **2017**, *102*, 2039–2047. [[CrossRef](#)]
20. Yang, Y.; Gao, X.; Zhang, M.; Yan, S.; Sun, C.; Xiao, F.; Huang, N.; Yang, X.; Zhao, K.; Zhou, H.; et al. Novel Role of FBXW7 Circular RNA in Repressing Glioma Tumorigenesis. *J. Natl. Cancer Inst.* **2018**, *110*, 304–315. [[CrossRef](#)]
21. Wang, F.; Nazarali, A.J.; Ji, S. Circular RNAs as potential biomarkers for cancer diagnosis and therapy. *Am. J. Cancer Res.* **2016**, *6*, 1167–1176. [[PubMed](#)]
22. Li, J.; Yang, J.; Zhou, P.; Le, Y.; Zhou, C.; Wang, S.; Xu, D.; Lin, H.-K.; Gong, Z. Circular RNAs in cancer: Novel insights into origins, properties, functions and implications. *Am. J. Cancer Res.* **2015**, *5*, 472–480. [[PubMed](#)]
23. Anastasiadou, E.; Jacob, L.S.; Slack, F.J. Non-coding RNA networks in cancer. *Nat. Rev. Cancer* **2018**, *18*, 5. [[CrossRef](#)] [[PubMed](#)]
24. Li, L.J.; Huang, Q.; Pan, H.F.; Ye, D.Q. Circular RNAs and systemic lupus erythematosus. *Exp. Cell Res.* **2016**, *346*, 248–254. [[CrossRef](#)] [[PubMed](#)]
25. Cardamone, G.; Paraboschi, E.M.; Rimoldi, V.; Duga, S.; Soldà, G.; Asselta, R. The characterization of GSDMB splicing and backsplicing profiles identifies novel isoforms and a circular RNA that are dysregulated in multiple sclerosis. *Int. J. Mol. Sci.* **2017**, *18*, 576. [[CrossRef](#)] [[PubMed](#)]
26. Burd, C.E.; Jeck, W.R.; Liu, Y.; Sanoff, H.K.; Wang, Z.; Sharpless, N.E. Expression of linear and novel circular forms of an INK4/ARF-associated non-coding RNA correlates with atherosclerosis risk. *PLoS Genet.* **2010**, *6*, e1001233. [[CrossRef](#)]
27. Lukiw, W.J. Circular RNA (circRNA) in Alzheimer’s disease (AD). *Front. Genet.* **2013**, *4*, 307. [[CrossRef](#)]
28. Ashwal-Fluss, R.; Meyer, M.; Pamudurti, N.R.; Ivanov, A.; Bartok, O.; Hanan, M.; Evantal, N.; Memczak, S.; Rajewsky, N.; Kadener, S. CircRNA Biogenesis competes with Pre-mRNA splicing. *Mol. Cell* **2014**, *56*, 55–66. [[CrossRef](#)]
29. Memczak, S.; Jens, M.; Elefsinioti, A.; Torti, F.; Krueger, J.; Rybak, A.; Maier, L.; Mackowiak, S.D.; Gregersen, L.H.; Munschauer, M.; et al. Circular RNAs are a large class of animal RNAs with regulatory potency. *Nature* **2013**, *495*, 333–338. [[CrossRef](#)]
30. Gao, Y.; Wang, J.; Zhao, F. CIRI: An efficient and unbiased algorithm for de novo circular RNA identification. *Genome Biol.* **2015**, *16*, 4. [[CrossRef](#)]
31. Westholm, J.O.; Miura, P.; Olson, S.; Shenker, S.; Joseph, B.; Sanfilippo, P.; Celniker, S.E.; Graveley, B.R.; Lai, E.C. Genome-wide Analysis of Drosophila Circular RNAs Reveals Their Structural and Sequence Properties and Age-Dependent Neural Accumulation. *Cell Rep.* **2014**, *9*, 1966–1980. [[CrossRef](#)] [[PubMed](#)]
32. Cheng, J.; Metge, F.; Dieterich, C. Specific identification and quantification of circular RNAs from sequencing data. *Bioinformatics* **2016**, *32*, 1094–1096. [[CrossRef](#)] [[PubMed](#)]
33. Zheng, Y.; Ji, P.; Chen, S.; Hou, L.; Zhao, F. Reconstruction of full-length circular RNAs enables isoform-level quantification. *Genome Med.* **2019**, *11*, 2. [[CrossRef](#)] [[PubMed](#)]
34. Metge, F.; Czaja-Hasse, L.F.; Reinhardt, R.; Dieterich, C. FUCHS-towards full circular RNA characterization using RNAseq. *PeerJ* **2017**, *5*, e2934. [[CrossRef](#)] [[PubMed](#)]
35. Hossain, M.T.; Peng, Y.; Feng, S.; Wei, Y. FcircSEC: An R Package for Full-length circRNA Sequence Extraction and Classification. *Int. J. Genom.* **2020**, *2020*, 9084901. [[CrossRef](#)]
36. Zhang, J.; Hou, L.; Zuo, Z.; Ji, P.; Zhang, X.; Xue, Y.; Zhao, F. Comprehensive profiling of circular RNAs with nanopore sequencing and CIRI-long. *Nat. Biotechnol.* **2021**, *39*, 836–845. [[CrossRef](#)]
37. Li, H.; Durbin, R. Fast and accurate short read alignment with Burrows-Wheeler transform. *Bioinformatics* **2009**, *25*, 1754–1760. [[CrossRef](#)]
38. Dobin, A.; Davis, C.A.; Schlesinger, F.; Drenkow, J.; Zaleski, C.; Jha, S.; Batut, P.; Chaisson, M.; Gingeras, T.R. STAR: Ultrafast universal RNA-seq aligner. *Bioinformatics* **2013**, *29*, 15–21. [[CrossRef](#)]